nature energy

SUPPLEMENTARY INFORMATION

https://doi.org/10.1038/s41560-020-0602-0

In the format provided by the authors and unedited.

Exploiting intervalley scattering to harness hot carriers in III–V solar cells

Hamidreza Esmaielpour[1,3], Kyle R. Dorman[1], David K. Ferry[2], Tetsuya D. Mishima[1], Michael B. Santos[1], Vincent R. Whiteside[1] and Ian R. Sellers[1]✉

[1]Homer L. Dodge Department of Physics & Astronomy, University of Oklahoma, Norman, OK, USA. [2]School of Electrical, Computer and Energy Engineering, Arizona State University, Tempe, AZ, USA. [3]Present address: Institut Photovoltaique d'Ile de France (IPVF), Palaiseau, France. ✉e-mail: sellers@ou.edu

Supplementary Information

Exploiting Intervalley Scattering to Harness Hot Carriers in III-V Solar Cells

Hamidreza Esmaielpour[1], Kyle R. Dorman[1], David K. Ferry[2], Tetsuya D. Mishima[1], Michael B. Santos[1], Vincent R. Whiteside[1], and Ian R. Sellers[1*]

[1] *Homer L. Dodge Department of Physics & Astronomy, University of Oklahoma, Norman OK 73019, U.S.A.*

[2] *School of Electrical, Computer, and Energy Engineering, Arizona State University, Tempe, AZ 85287, U.S.A.*

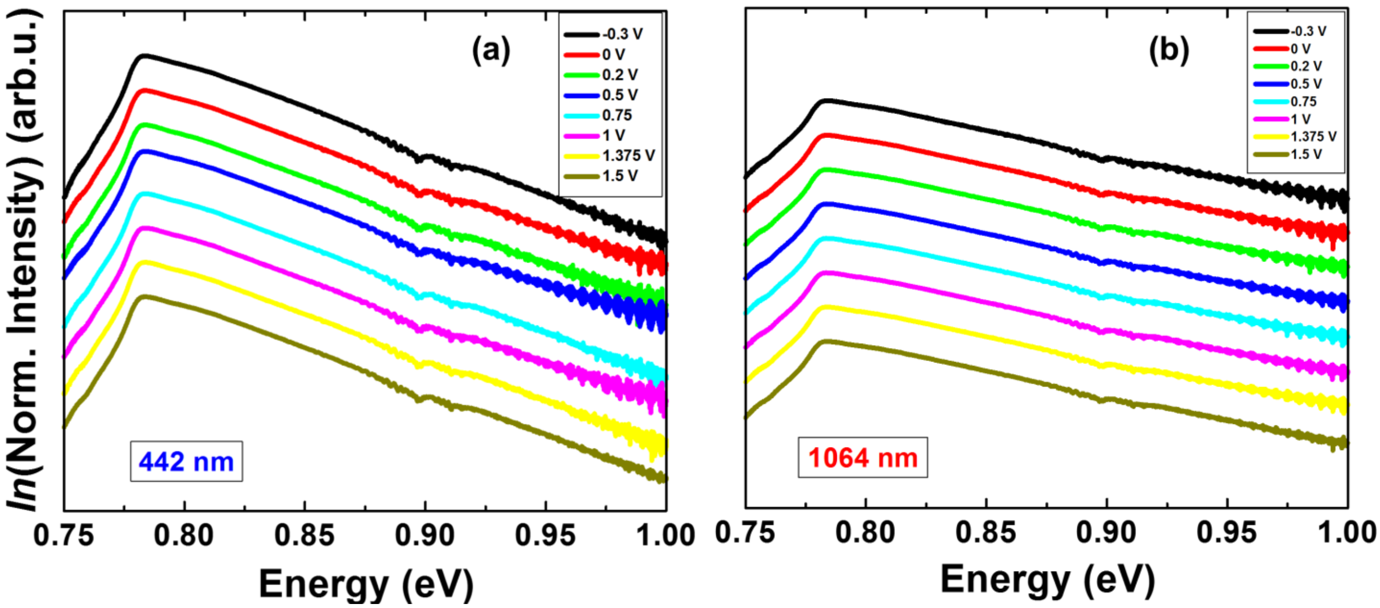

Supplementary Figure 1: Bias dependent Photoluminescence (PL) spectra recorded at 300 K
Bias dependent Photoluminescence (PL) spectra recorded at 300 K for (a) visible (442 nm) and (b) infrared (1064 nm) excitation, respectively. The PL data were measured using the same (constant) absorbed power – as determined by the maximum saturation current in the respective monochromatic current density-voltage (J-V) responses as shown in Figures 3(a) and (b) of the manuscript. The carrier temperature difference, ΔT was extracted at several bias ranges between -0.3 V to 1.5 V to extract/probe ΔT at the operating conditions observed across the monochromatic current-density-voltage (*J*-*V*) curves under the respective excitation wavelengths. In both cases (visible and IR) the high energy tail is essentially constant as a function of bias reflecting the independence of ΔT for both excitation wavelengths as shown in Figure 3(c).

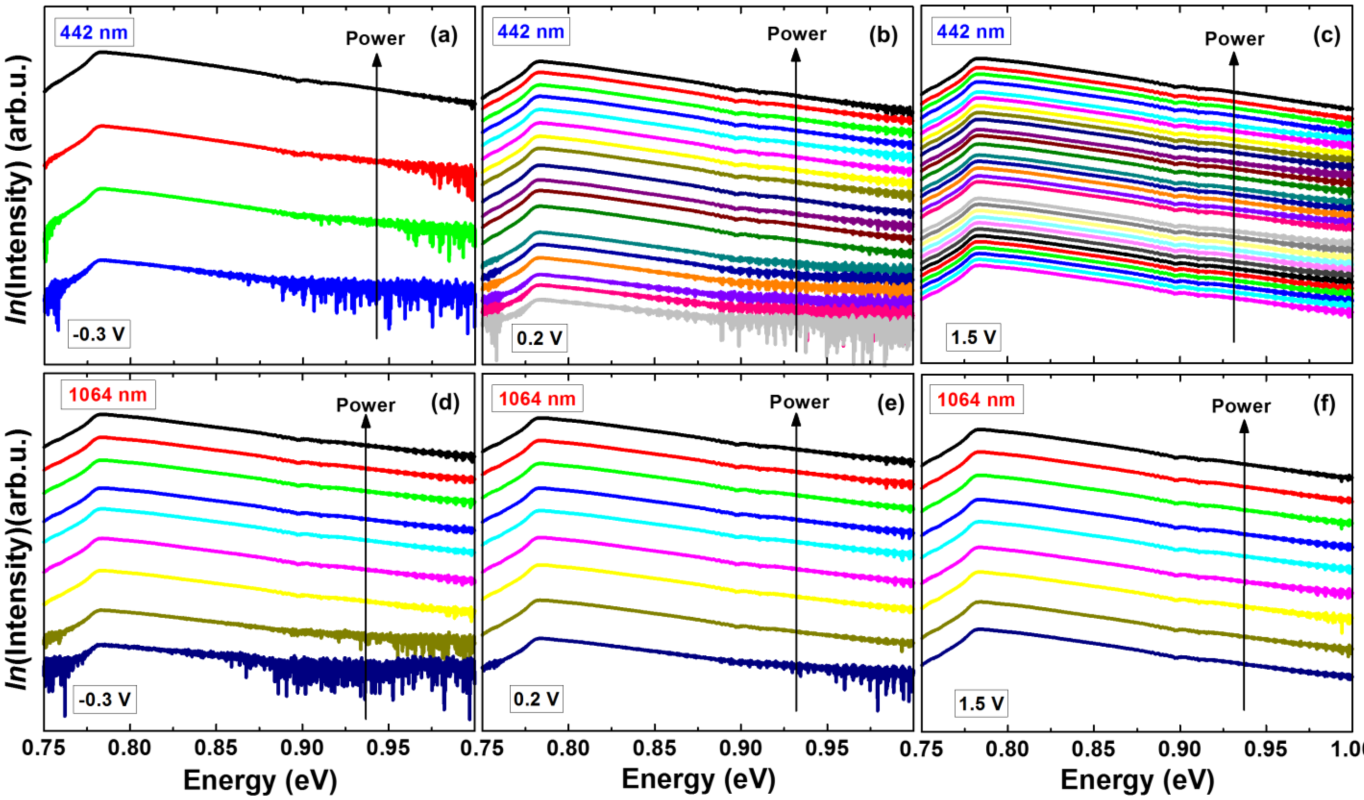

Supplementary Figure 2: Power dependent photoluminescence spectra at fixed biases

Power dependent photoluminescence spectra at fixed biases of -0.3 V, 0.2 V, and 1.5 V under blue (442 nm) and IR (1064 nm) excitation. These data represent the spectra used to extract the power dependent carrier temperature, ΔT shown in Supplementary Figure(s) 3(a), (b), and (c). The (absorbed) power ranges used were matched over low absolute power ranges of 1 mW to 32 mW (using the saturated current extracted from the simultaneous *J-V* under monochromatic excitation). (a,d), (b,e), and (c,f) show the power dependent PL at fixed voltages of: – 0.3 V, 0.2 V, and 1.5 V, for 442 nm, 1064 nm respectively. These voltages were chosen since they reflect specific regions in the *J-V* response in which the carrier transport changes from field aided minority electrons, inhibited minority electrons, and majority electrons in the forward operating regime.

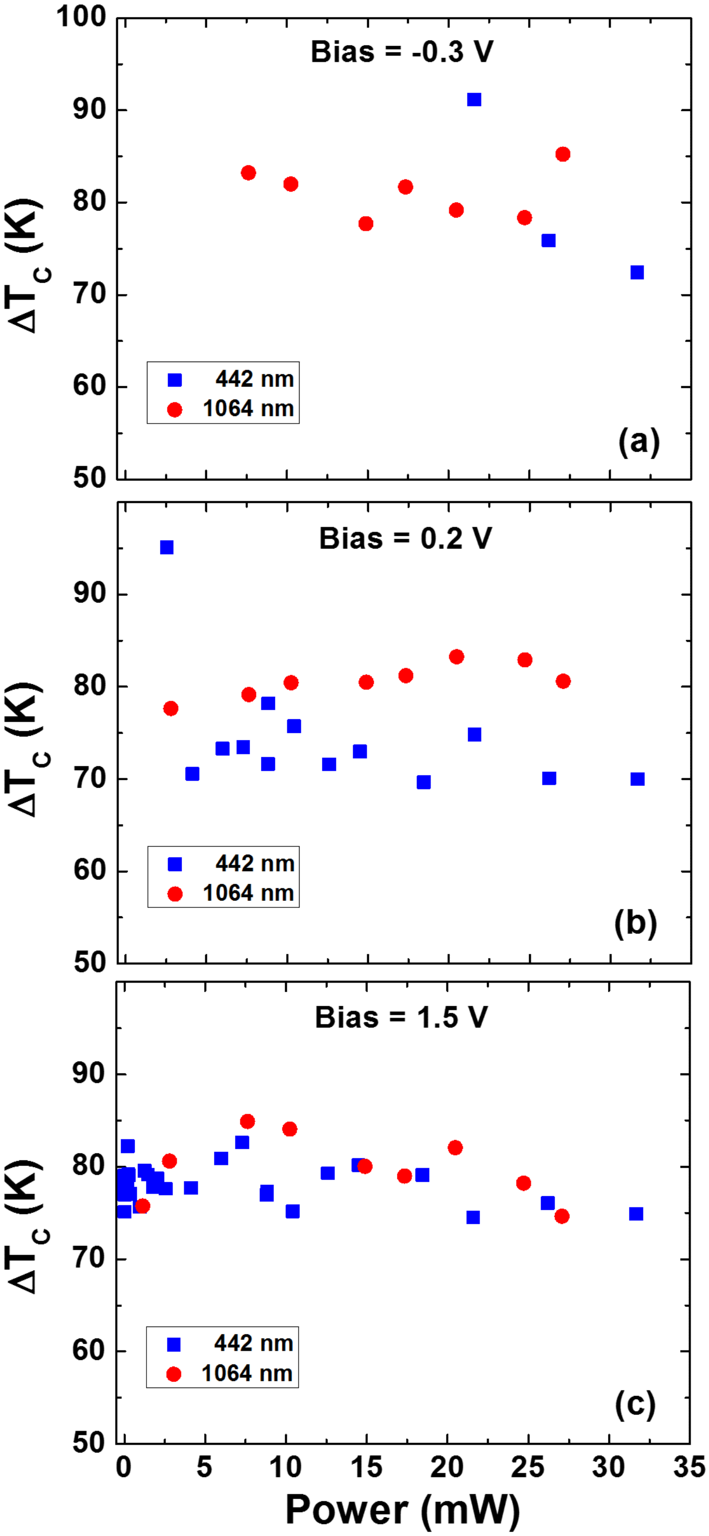

Supplementary Figure 3: Power dependent *ΔT* at fixed biases

Power dependent *ΔT* at fixed biases: (a) at -0.3 V, (b) at 0.2 V, and (c) at 1.5 V.

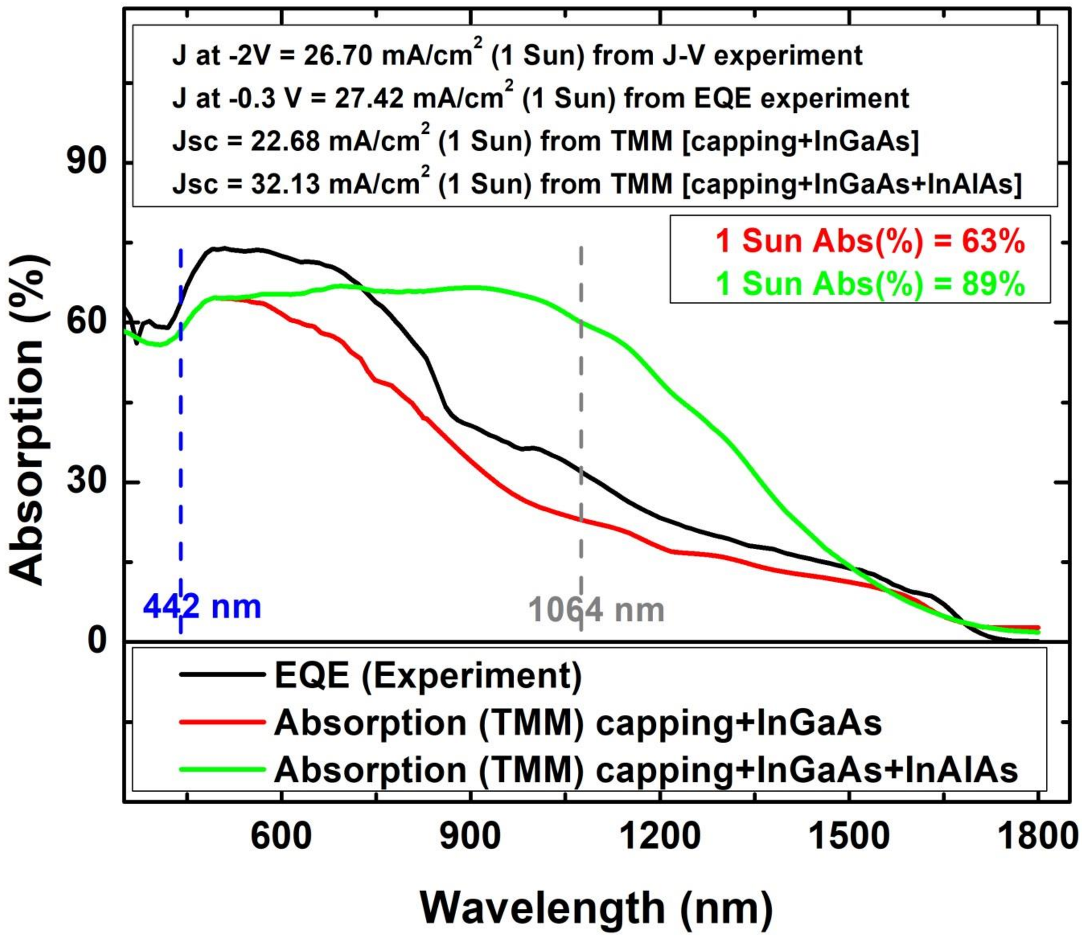

Supplementary Figure 4: Transfer matrix (TM) calculations

Transfer matrix (TM) calculations showing the total predicted absorption under 1-sun AM 1.5G excitation for the InGaAs/AlInAs device under investigation. These Mathematica calculations consider surface reflectivity and transmission losses at the front and all subsequent interface layers within the structure. The total calculated absorption in the upper AlInAs cap/barrier and InGaAs absorber is shown in red, contributing an absorption of ~ 63% of the unreflected incident solar irradiations, which translates to a total short circuit density (J_{sc}) of ~ 22.7 mA/cm^2. Including the p-AlInAs base/buffer region increases this value to 89% (green), and a J_{sc} ~ 32.1 mA/cm^2. Also shown in black in this Supplementary Figure 4 is the experimentally measured external quantum efficiency (EQE) at 300 K. The measured EQE follows closely that of the calculated absorption of the absorber demonstrating the important role of carrier extraction in this layer, and the limited total absorption of the relatively thin (250 nm) InGaAs absorber in this device. Also included in the caption are the J_{sc} or maximum current densities values at the saturation points (-0.3 V), and under strong reverse bias (-2 V). The values of ~ 27 mA/cm^2 extracted for these biases reflects the total current generated in the active absorber (maximum photogenerated current), suggesting that most of the current absorbed in the InGaAs is harnessed in reverse bias in these systems demonstrating the high material quality of the sample measured.

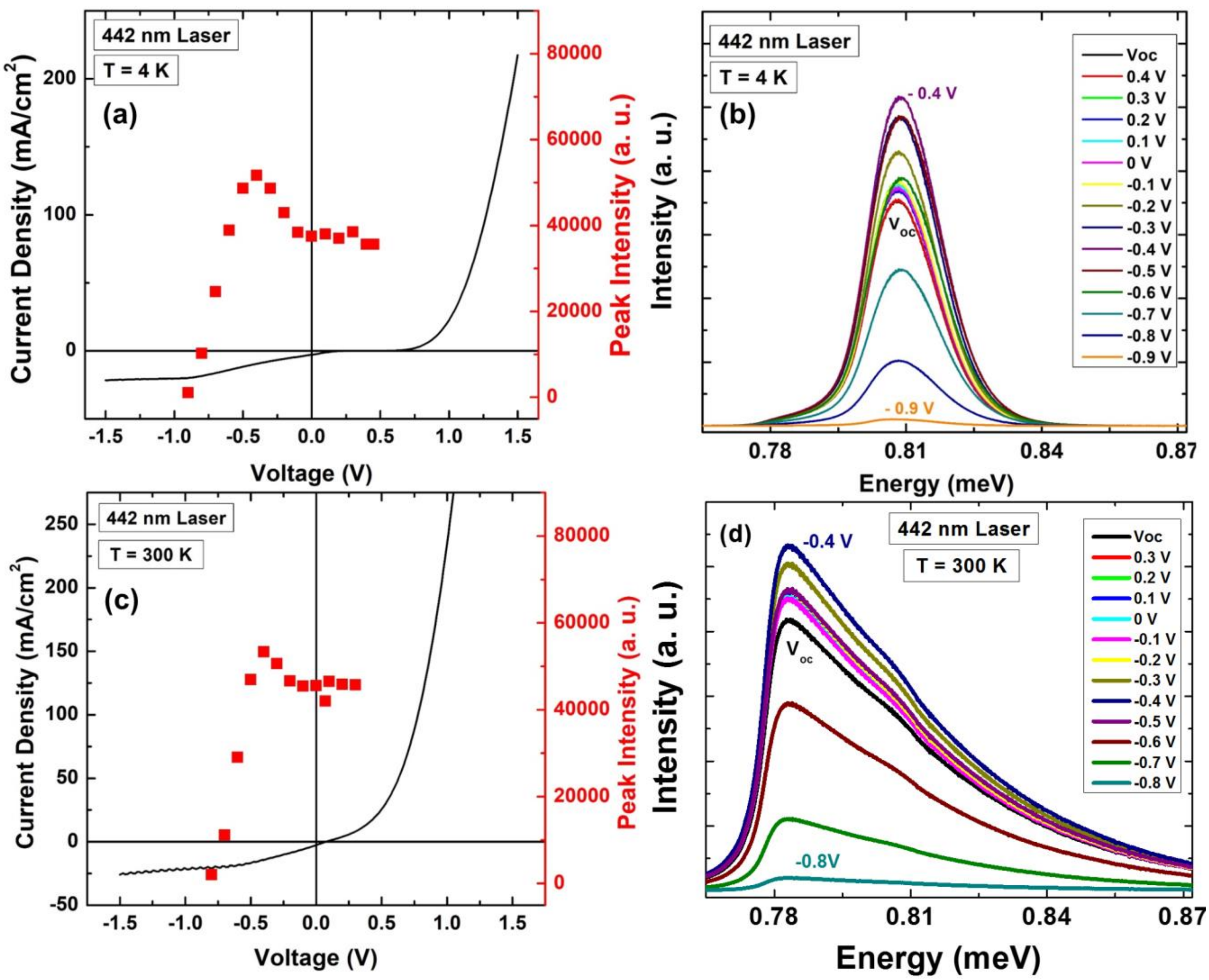

Supplementary Figure 5: Monochromatic J-V and bias dependent PL under 442 nm excitation
(a) Comparison of monochromatic J-V under 442 nm excitation and the peak intensity of the bias dependent PL between -0.9 V and 0.4 V, at 4.2 K. In this Figure the PL (solid red squares) remains approximately constant at biases above -0.1 V. However, the peak PL increases as the bias is reduced and approaches the saturation current in the *J-V* (~ -0.4 V). This increase in PL efficiency reflects the build-up of photogenerated minority electrons at the upper n^+-AlInAs/n-InGaAs interface, where these (blue excited) carriers experience a barrier due to the mismatch in the valley degeneracy across the interface. These carriers subsequently relax to the ground state (Γ) at the interface, preferentially recombining with holes at the band gap, therefore emitting stronger PL. This effect is both temperature and (excitation) power dependent, with the large build-up of charges at the interface perturbing the electric field across at the absorber/barrier interface and the relative confinement potential. As the reverse bias is increased further, the tunneling of carriers from the absorber dominates thus, the current density increases to saturation along with a simultaneous decrease in the PL intensity (above ~ - 0.4 V). The PL spectra at the various biases for those data shown in (a) are shown in (b). A comparison of the monochromatic (blue - 442 nm) J-V and bias dependent peak PL intensity at 300 K is shown in (c). The associated PL spectra are shown in (d). Evidence of a bias dependent barrier to carrier extraction and correlated PL emission is also clear at room temperature.

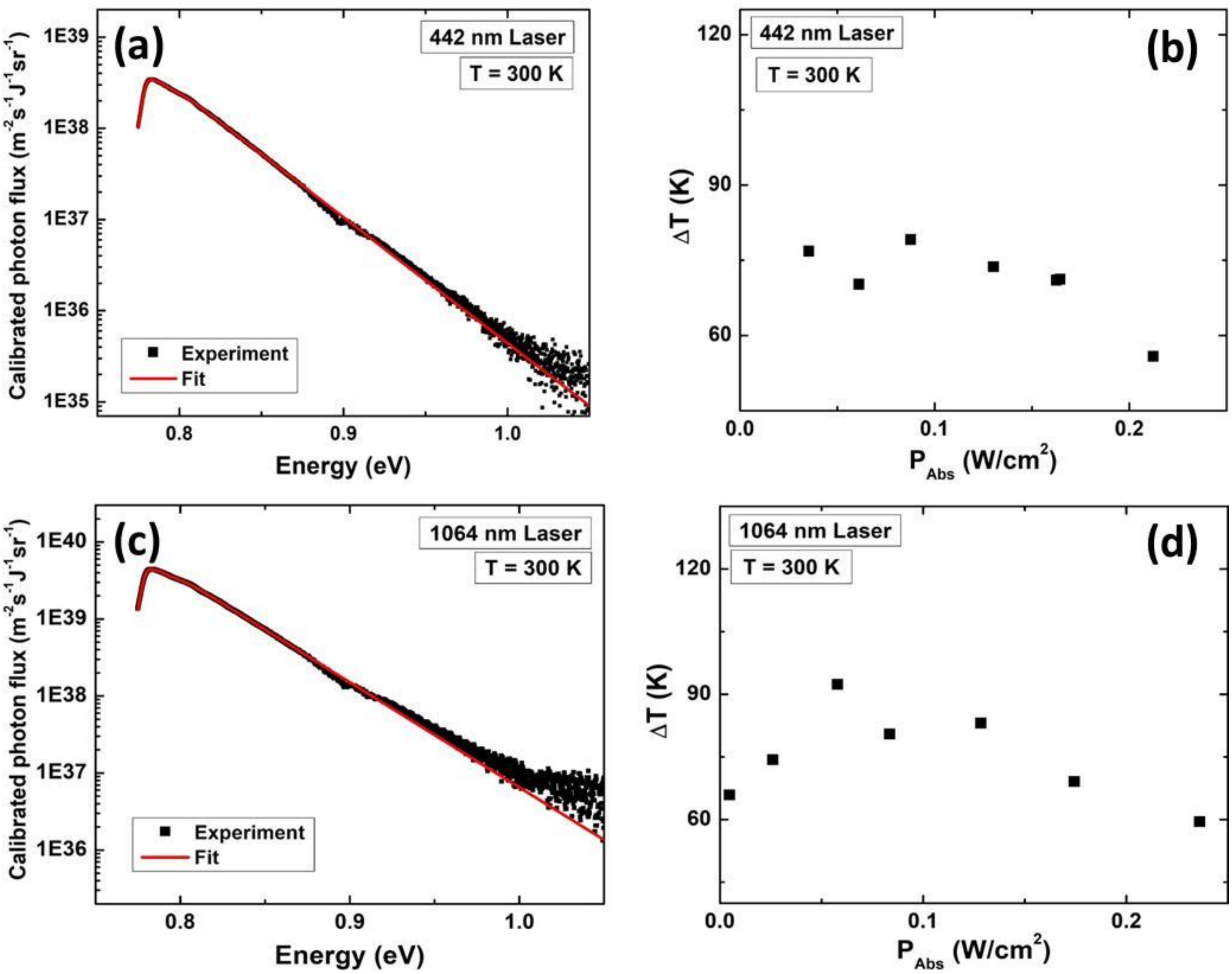

Supplementary Figure 6. **Full spectral fit of the power dependent PL at 300 K**
Full spectral fit of the power dependent PL at 300 K using the method of [1] and [2] for (a) excitation using the 442 nm and (c) 1064 nm laser at compatible absorbed power. The extracted power dependent carrier temperature difference(s), ΔT, are shown in (b) 442 nm and (d) 1064 nm, respectively. The ΔT values extracted are well matched to those determined using simple linear fitting to the high energy tail using Equation (1) discussed in Methods: Carrier temperature determination use generalized Planck equation of the manuscript and shown in Figure(s) 2(c) and (f), respectively. This comparison demonstrates the validity of the simple analysis implemented in the manuscript with respect to bulk materials.

Supplementary Note 1: Power dependent *ΔT* at fixed biases

Supplementary Figure 3(a) shows the power dependence of *ΔT* at a reverse bias of -0.3 V. Under this (reverse) bias the field aided extraction results in maximum carrier collection and a saturated photogenerated *J*-*V* response. The reverse bias has two effects: 1) to sweep the photoexcited electrons and holes out of the absorber towards the *n* and *p* contacts, respectively; and 2) to facilitate electron tunneling out of the absorber into the n-AlInAs layer.

Regarding the first point, the large electric field across the absorber (~ 42 kV/cm) will accelerate the photogenerated carriers, facilitating the scattering of electrons from the Γ-valley to the L- and X-valleys (see Figure 1(d)). Supplementary Figure 3(a) shows ΔT at -0.3 V. Although one might expect the presence of hot carrier extraction at high energy excitation, high in the Γ-valley and above the AlInAs energy, the lower energy photoexcited carriers absorbed below both the L-valley energy of the InGaAs and the AlInAs barrier would (to first order) be expected to be at equilibrium, thermalized, and therefore not "hot." However, if these carriers experience a high electric field, they gain kinetic energy and are therefore also scattered to the upper valleys. The presence of hot carriers generated by the 1064 nm laser (solid red circles) at the same temperature as those scattered at higher energy (442 nm, solid blue squares) demonstrates the potential of manipulating the internal electric field to extract low energy carriers at -0.3 V and to develop solar cells with operating voltages that are defined for all wavelengths by the upper valley energies in the absorber, not by the band gap.

Supplementary Figure 3(b) shows the power dependence of ΔT at a forward bias of 0.2 V, which lies within the solar cell photovoltaic (operating) regime but near the inflection point of the *J-V* response observed at 1-sun (Figure 3(c)), as well as under monochromatic illumination. This inflection point is both power and temperature dependent and reflects the valley degeneracy across the InGaAs/n-AlInAs interface. Specifically, the L-valley in the InGaAs is aligned with the Γ-valley in the AlInAs as shown schematically in Figures 2(a) and 2(d). This property results in a barrier to hot carrier extraction, since the transfer of carriers from the higher mass L-valley (InGaAs) to the lower mass Γ-valley is a slower process than the process, which scattered and stored the high energy photogenerated carriers in the first place. Despite the inhibited collection and reduced fill factor at 0.2 V, the ΔT presented in Supplementary Figure 3(b) remains essentially both power and excitation wavelength independent, demonstrating the presence of IV scattering for all photogenerated carriers. Supplementary Figure 3(b) also indicates that despite the reduction in electric field across the active region under this relatively low forward bias (0.2 V), this field remains strong enough for almost complete scattering of lower energy IR (1064 nm) generated carriers into the upper valleys.

Supplementary Figure 3(c) shows the power dependence of ΔT at +1.5 V, well above the turn on voltage for this device (~1.38 V). Despite the apparent absence of an internal electric field, a power independent ΔT of ~ 70 K is evident for the PL for both the blue (442 nm) and the IR (1064 nm) excitation.

Supplementary References

[1] F. Gibelli, L. Lombez, and J-F. Guillemoles. "Accurate radiation temperature and chemical potential from quantitative photoluminescence analysis of hot carrier populations." *Journal of Physics: Condensed Matter* vol. 29 p 06LT02, 2016

[2] V. R. Whiteside *et al*. "The role of intervalley scattering in hot carrier transfer and extraction in type-II InAs/AlAsSb quantum well solar cells," *Semiconductor Science & Technology*, vol. 34, p094001, 2019